

Research Article

Facile Preparation and Photoinduced Superhydrophilicity of Highly Ordered Sodium-Free Titanate Nanotube Films by Electrophoretic Deposition

Minghua Zhou^{1,2} and Huogen Yu²

¹Lab of Medical Chemistry, Hubei University of Medicine, Hubei, Shiyan 442000, China

²Department of Chemistry, School of Science, Wuhan University of Technology, Wuhan 430070, China

Correspondence should be addressed to Huogen Yu, yuhuogen@yahoo.cn

Received 30 December 2011; Accepted 9 January 2012

Academic Editor: Baibiao Huang

Copyright © 2012 M. Zhou and H. Yu. This is an open access article distributed under the Creative Commons Attribution License, which permits unrestricted use, distribution, and reproduction in any medium, provided the original work is properly cited.

Highly ordered sodium-free titanate nanotube films were one-step prepared on F-doped SnO₂-coated (FTO) glass via an electrophoretic deposition method by using sodium titanate nanotubes as the precursor. It was found that the self-assembled formation of highly ordered sodium titanate nanotube films was accompanied with the effective removal of sodium ions in the nanotubes during the electrophoretic deposition process, resulting in the final formation of protonated titanate nanotube film. With increasing calcination temperature, the amorphous TiO₂ phase is formed by a dehydration process of the protonated titanate nanotubes at 300°C and further transforms into anatase TiO₂ when the calcination temperature is higher than 400°C. Compared with the as-prepared titanate nanotube film, the calcined titanate nanotube film (300–600°C) exhibits attractive photoinduced superhydrophilicity under UV-light irradiation. In particular, 500°C-calcined films show the best photoinduced superhydrophilicity, probably due to synergistic effects of enhanced crystallization, surface roughness, and ordered structures of the films.

1. Introduction

Among various oxide semiconductors, titania appears promising and important for the use in environmental purification due to its strong oxidizing power, nontoxicity and long-term photostability [1–10]. In addition to the conventional photocatalytic activity, photoinduced superhydrophilic properties of two-dimensional (2D) TiO₂ thin films have attracted much attention in recent years [11–13]. By utilizing the superhydrophilic surface of TiO₂ thin films, we can develop antifogging or self-cleaning glass, mirrors, and other ecological building materials [14, 15]. However, the further enhanced photoinduced hydrophilicity is necessary for practical uses. To achieve this goal, great attentions should be focused on the textural design of the 2D TiO₂ thin films.

Recently, titanate-based films have been intensively investigated due to the large specific surface areas and unique structural features [16–23]. For example, Tian et al. [16] reported a simple hydrothermal and seeded growth process to fabricate titanate nanotube film by directly immersing

Ti substrate in concentrated NaOH solution for certain time. Tokudome and Miyauchi [17] developed a layer-by-layer growth technique to prepare thin titanate nanotube films. Nevertheless, the construction of the titanate nanotube films with controllable textures is still remained as a great challenge, and alternative techniques for films are highly desirable. Recently, electrophoretic deposition (EPD) was successfully developed to fabricate various thin-film materials [18–20]. There are many advantages of this technique over other deposition methods. For example, higher deposition rate can be easily achieved with a quick deposition, in addition to its reproducibility of deposition. It is also an efficient technique to control the thickness and morphology of the films by controlling current or potential. Specially, the EPD has a flexibility of depositing films on different shapes and sizes and can be extended to a large scale for commercial applications. Another advantage of this method is that it can be carried out at room temperature, thereby reducing the possibility of deterioration of the surrounding.

Here, we developed the EPD method for constructing ordered titanate nanotube films using preformed titanate

nanotubes as raw materials. The effects of calcination temperatures on the surface morphology, microstructures, as well as the properties of superhydrophilicity were studied. It was demonstrated that the calcination of those titanate nanotube films above 300°C converted into ordered TiO₂ nanorod films with attractive photoinduced superhydrophilicity.

2. Experimental

2.1. Preparation of Samples. Sodium titanate nanotubes were prepared according to our previous reported methods [24, 25]. TiO₂ source used for the titanate nanotubes was commercial-grade TiO₂ powder (P25, Degussa AG, Germany) with crystalline structure of ca. 20% rutile and ca. 80% anatase and primary particle size of ca. 30 nm. In a typical preparation, 1.5 g of the TiO₂ powder was mixed with 140 mL of 10 M NaOH solution, followed by hydrothermal treatment of the mixture at 150°C in a 200 mL Teflon-lined autoclave for 48 h. After hydrothermal reaction, the precipitate was separated by filtration and washed with distilled water for three times. The washed samples were dried in a vacuum oven at 80°C for 8 h.

Ordered titanate nanotube films were deposited on FTO glass using a modified EPD technique [18, 20]. The pH of electrolyte solution is adjusted to about 9.0 using ammonia. The isoelectric point of titanate nanotubes was about 5.5, which was lower than that of electrolyte solution. Therefore, titanate nanotubes are negatively charged particles at pH 9. During EPD, the cleaned FTO glass was kept at positive potential (anode) while pure silver (Ag) foil was used as counter (cathode) electrode. The EPD was carried out at a voltage of 10.0 ± 0.10 V (current up to 0.01 A), and deposition time was 20 min. Subsequently, the coated films were rinsed with distilled water, dried in air, and calcined at 300, 400, 500, and 600°C in air for 1 h, respectively.

2.2. Characterization. Morphology observation was performed on S-4800 field emission scanning electron microscope (FESEM, Hitachi, Japan). X-ray diffraction (XRD) patterns were obtained on a D/MAX-RB X-ray diffractometer (Rigaku, Japan). Transmission electron microscopy (TEM) analyses were conducted with a JEM-2010F electron microscope (JEOL, Japan). X-ray photoelectron spectroscopy (XPS) measurements were done with a Kratos XSAM800 XPS system; all the binding energies were referenced to the C1s peak at 284.8 eV of the surface adventitious carbon.

2.3. Hydrophilicity Test. The sessile drop method was used for the measurements of water contact angle (θ) on the surface of as-prepared films with a contact angle meter (JC2000A, China) [14, 15]. The droplet size used for each measurement was 3 μ L. Water droplets were placed at five different positions of each film, and the average value was adopted as the contact angle.

2.4. Hydroxyl Radical Analysis. The formation of hydroxyl radical ($\bullet\text{OH}$) on the surface of photoilluminated as-prepared films was detected by photoluminescence (PL)

technique using terephthalic acid (TA) as a probe molecule. TA readily reacts with $\bullet\text{OH}$ to produce highly fluorescent product, 2-hydroxyterephthalic acid (TAOH) [26, 27]. PL spectra of generated TAOH were measured on a Fluorescence Spectrophotometer (F-7000, Hitachi, Japan) using a excitation wavelength 315 nm at a scan speed of 1200 nm min⁻¹ with the PMT voltage of 700 V. The width of excitation slit and emission slit was 1.0 nm.

3. Results and Discussion

Figure 1(a) shows the SEM image of the as-prepared titanate nanotube powder prepared by a hydrothermal process, indicating that the titanate nanotube shows a diameter of 7–15 nm and a length of several hundred nanometers. The TEM image (inset in Figure 1(a)) clearly indicates that the as-prepared nanotubes possess a uniform inner and outer diameter along their length. The corresponding XRD pattern of the titanate nanotubes is shown in Figure 2(a). The diffraction peak at around 10° is due to the layered structure of nanotubes along their radial direction, while other diffraction peaks at around 24°, 28°, and 48° are related to the sodium titanate phase. Therefore, the as-prepared sample can be ascribed to sodium titanate nanotubes.

When the sodium titanate nanotubes were deposited on the surface of FTO substrate by EPD method, it is interesting to find that the as-prepared films show an ordered assembled structure of the nanotubes along their long-axis direction (Figure 1(b)). Moreover, in addition to the diffraction peaks of FTO, only one diffraction peak at ca. 10° can be observed and other peaks at ca. 24°, 28°, and 48° are completely disappeared (Figure 2(b)). This indicates that the phase structure of the nanotubes is changed while the layered structure of nanotubes is well preserved after EPD. To further investigate the phase structure and element composition of the ordered films, XPS analysis was performed and shown in Figure 3. It can be seen that the sodium titanate nanotube powders (Figure 3(a)) contain Ti, O, C, and Na elements, with sharp photoelectron peaks appearing at binding energies of 458 (Ti 2p), 531 (O 1s), 285 (C 1s), and 1071 eV (Na 1s), respectively. The carbon peak is attributed to the adventitious hydrocarbon from XPS instrument itself. After the sodium titanate nanotube powder is deposited on the surface of FTO to form a film, it is found that no XPS peaks corresponding to Na element are recorded in the as-prepared film (Figure 3(b)). These results indicate that EPD is an effective way to remove the intercalated sodium in the sodium titanate nanotubes and the Na⁺ can be detached from the nanotube when the nanotubes move towards anode and are coated on the surface of FTO during EPD, which is in good agreement with the previous studies [28]. Therefore, the phase structure of highly ordered film can be attributed to protonated titanate with a similar crystal structure of H₂Ti₃O₇ [29, 30] and H_xTi_{2-x/4}O₄(x = 0.75) [31].

Using a simple hydrothermal treatment of crystalline TiO₂ particles with NaOH aqueous solutions, high-quality nanotubes with uniform diameter of around 7–15 nm were obtained and their specific surface area reached more than 400.0 m²/g [24]. Unfortunately, the obtained nanotubes are

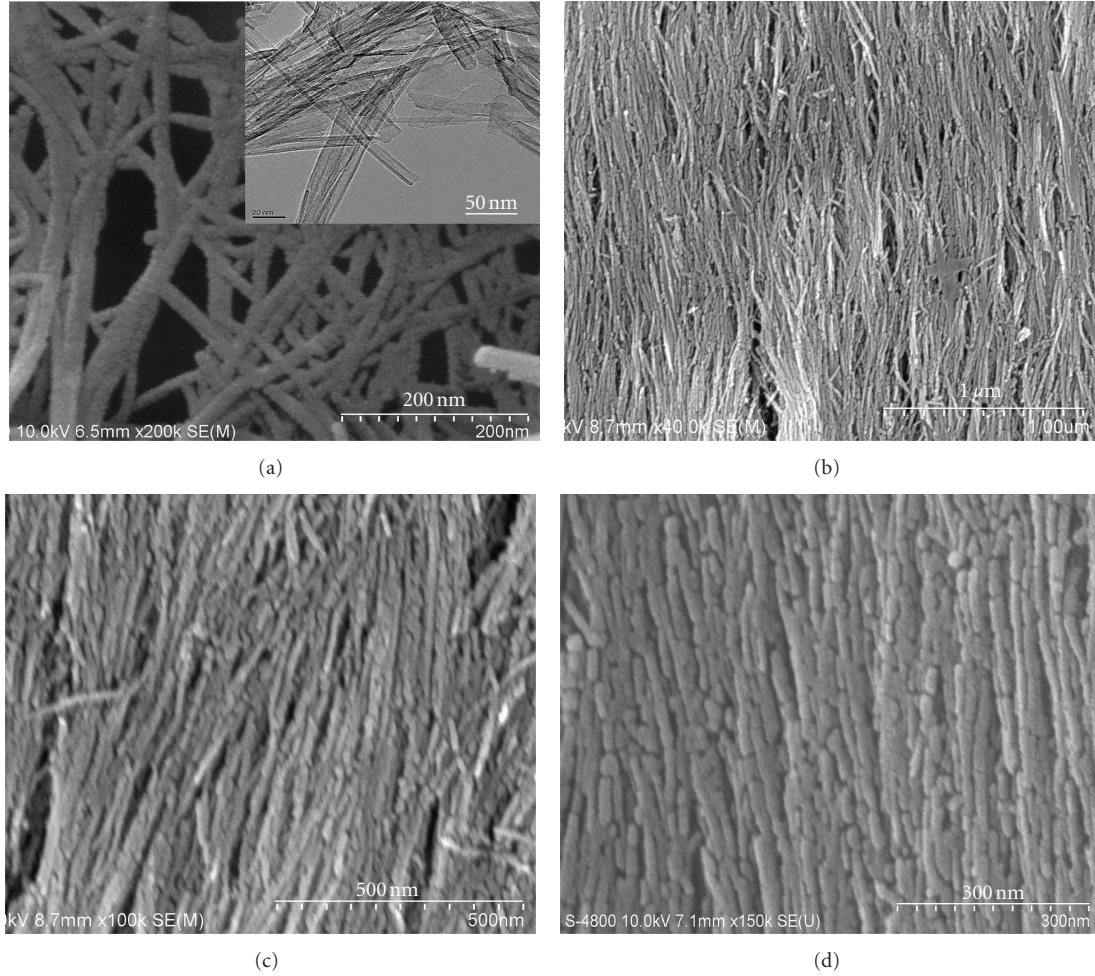


FIGURE 1: FESEM images of (a) as-prepared sodium titanate nanotube powders, (b) as-prepared titanate nanotube films, (c) 300°C-calcined titanate nanotube films, and (d) 500°C-calcined titanate nanotube films. Inset in (a) is the corresponding TEM image.

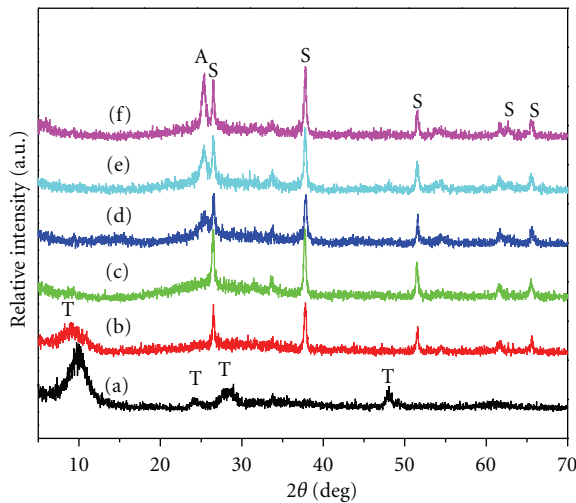


FIGURE 2: XRD patterns of the (a) as-prepared sodium titanate nanotube powders, (b) as-prepared titanate nanotube films, and after calcination at (c) 300°C, (d) 400°C, (e) 500°C, and (f) 600°C. The labeled S, T, and A are related to crystal phase of SnO₂, titanate nanotube, and anatase TiO₂, respectively.

sodium titanate phase and showed no photocatalytic activity in our previous experiments [24, 25]. To prepare the high-active photocatalyst, the sodium titanate nanotubes should be carefully washed with HCl solution to remove the sodium ions intercalated in the nanotubes. However, the above ion-exchange method is a time-wasting process and a lot of HCl solution is required [24, 25]. In this study, the EPD method provides a more effective and easy strategy for the removal of sodium in the titanate nanotubes. Based on the above results, it is clear that the self-assembly of highly ordered sodium titanate nanotube films was accompanied with the effective removal of sodium ions in the nanotubes during the EPD process, resulting in the final formation of protonated titanate nanotube film.

The effects of calcination temperature on the surface morphology of the titanate nanotube films are investigated. At 300°C, the calcined nanotube films still maintain a similar ordered morphology of self-assembled titanate nanotubes. However, some broken and short rods can be clearly observed (Figure 1(c)). According to the XRD results shown in Figure 2(c), no new diffraction peaks can be observed in addition to the substrate of FTO, suggesting the formation of

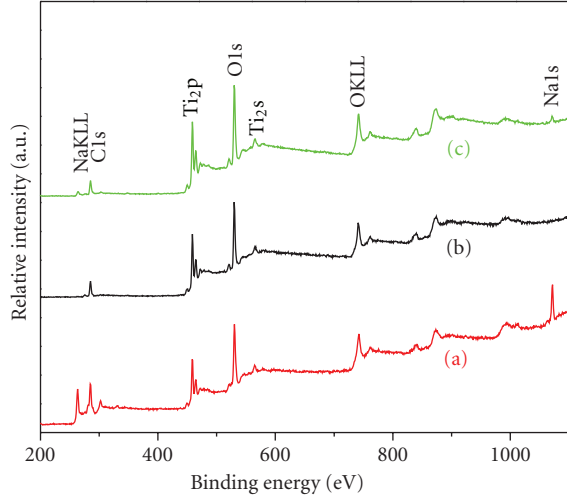


FIGURE 3: XPS survey spectra of (a) as-prepared sodium titanate nanotube powders, (b) as-prepared titanate nanotube films, and (c) 500°C-calcined titanate nanotube films.

amorphous phase after calcination at 300°C. Therefore, the formation of 300°C-calcined ordered structure (Figure 1(c)) is probably due to the phase transformation from titanate to amorphous TiO_2 . When the calcination temperature increases to 400°C (Figure 2(d)), the diffraction peak at ca. 25° is formed, indicating the further phase transformation from amorphous to anatase TiO_2 . With further increase of the calcination temperature to 500°C, the titanate nanotubes are transformed into anatase TiO_2 nanorods with a length of 20–70 nm (Figure 1(d)). When the calcination temperature is 600°C, both the one-dimensional structures and their ordered assemblies are completely destroyed (data not shown), while XRD patterns suggest that the film samples show an enhanced crystallization with increasing calcination temperature. On the other hand, it should be noted that, when the calcination temperature is over 500°C, the XPS peak of Na element (Figure 3(c)) at the binding energy of 1071 eV appears again, which is associated with the migration of some sodium ions from the FTO glass into the films surface during heat treatment, in good agreement with our previous results [32].

Figure 4 shows the changes of water contact angle for the titanate nanotube films before and after calcination at various temperatures. It can be seen that the water contact angles for all the freshly prepared films were about 5°. This may be attributed to the fact that all the freshly prepared films had a clear and roughened surface. However, when these film samples were stored in the dark in air for about 2 months, the water contact angles increased gradually to about 60~65° (Figure 4(a)). This is ascribed to the fact that the surface is contaminated by adsorbing some gaseous contaminants from air and the surface defect sites can be healed or replaced gradually by oxygen atoms, which changes the surface wettability from a superhydrophilic to a hydrophilic state [33]. From the viewpoint of practical use and commercialization, it would be more valuable if the superhydrophilicity of

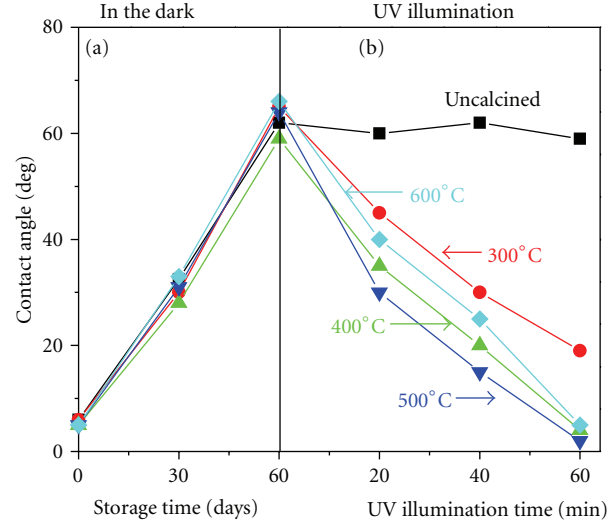
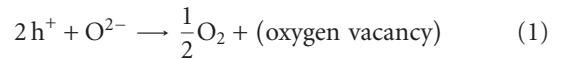


FIGURE 4: Changes in the water contact angle of the various titanate nanotube films: (a) stored in a dark room for 60 days and (b) subsequently illuminated by UV light for 60 min.

the films could be remained much longer. Fortunately, the superhydrophilicity of the calcined titanate nanotube films could be fully recovered by UV illumination (Figure 4(b)). However, the superhydrophilicity of the as-prepared titanate nanotube films cannot be recovered, suggesting that the conversion of those titanate nanotube films into ordered titania nanorods films upon calcination is significant for the recovering process. Moreover, the recovering rate of hydrophilicity of the calcined titanate nanotube films is obviously dependent on the calcination temperature. In particular, 500°C-calcined films show the best photoinduced superhydrophilicity. This may be related to the synergistic effects of enhanced crystallization, surface roughness, and orderly assembled structures of the films. The enhanced crystallization of anatase film is beneficial for the separation of photogenerated charge carriers and thus showing a better photocatalytic activity. The subsequent faster degradation of the surface-enriched pollutant molecules is an important factor responsible for the more rapid change of the surface to the superhydrophilic state. Moreover, the favored separation and diffusion of photogenerated charge carriers facilitates the transfer of the photogenerated holes towards lattice O^{2-} anions, creating more oxygen vacancies [33]:



Consequently, water molecules may coordinate into the oxygen vacancy sites, resulting in more abundant surface hydroxyl, which is confirmed to some extent by the greater formation rate of $\cdot\text{OH}$. The formation of $\cdot\text{OH}$ on the surface of the samples after UV irradiation can be detected by a PL technique using TA as a probe molecule (see below).

The ready reaction of photogenerated $\cdot\text{OH}$ with TA gave rise to highly fluorescent TAOH with typical PL signal centered at 425 nm. In addition, this PL intensity was proportional to the amount of $\cdot\text{OH}$ produced. Figure 5 showed

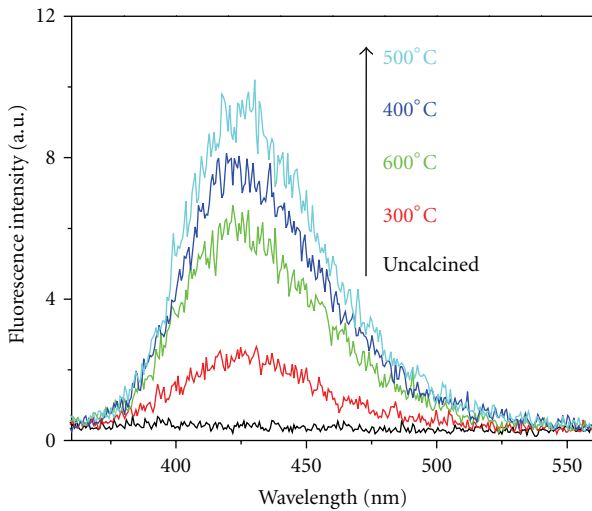


FIGURE 5: The fluorescence spectra related to formed fluorescent TAOH for the various films under UV-light irradiation at a fixed 60 min.

the PL spectra for the various samples at fixed irradiation time (60 min). Clearly, the order of the formation rate of •OH for these films is showed as follows: 500°C- > 400°C-> 600°C- > 300°C-calcined > uncalcined, which is consistent with the change rate of hydrophobic to hydrophilic state illustrated in Figure 4. In addition, the increased surface roughness coupled with abundant surface hydroxyl groups can adsorb and fix more water [15] to produce more •OH. Moreover, small micropores in the films can also produce a two-dimensional capillary phenomenon, which is supposed to be enhanced by the ordered assemblies of nanorod as reflected in Figure 1.

4. Conclusions

Highly ordered sodium-free titanate nanotube films were one-step prepared on FTO substrate via an EPD method by using sodium titanate nanotubes as the precursor. The self-assembled formation of highly ordered sodium titanate nanotube films was accompanied with the effective removal of sodium ions in the nanotubes during the EPD process, resulting in the final formation of protonated titanate nanotube film. The calcination temperature has an obvious effect on the morphology and photoinduced hydrophilicity of the titanate nanotube films. At 500°C, the prepared film shows the best photoinduced superhydrophilicity and the fastest formation rate of hydroxyl radicals, probably due to synergistic effects of good crystallization, surface roughness, and orderly assembled structures of the films.

Acknowledgments

This work was partially supported by the National Natural Science Foundation of China (20803055). This work was also supported by the Key Science Research Project of the Hubei Provincial Department of Education (D20112107),

the Science Research Project of Hubei University of Medicine (2009QDJ25), and the Fundamental Research Funds for the Central Universities (Grant 2011-1a-039).

References

- [1] M. R. Hoffmann, S. T. Martin, W. Choi, and D. W. Bahne-mann, "Environmental applications of semiconductor photocatalysis," *Chemical Reviews*, vol. 95, no. 1, pp. 69–96, 1995.
- [2] R. Asahi, T. Morikawa, T. Ohwaki, K. Aoki, and Y. Taga, "Visible-light photocatalysis in nitrogen-doped titanium oxides," *Science*, vol. 293, no. 5528, pp. 269–271, 2001.
- [3] H. Yu, H. Irie, Y. Shimodaira et al., "An efficient visible-light-sensitive Fe(III)-grafted TiO₂ photocatalyst," *Journal of Physical Chemistry C*, vol. 114, no. 39, pp. 16481–16487, 2010.
- [4] H. Yu, H. Irie, and K. Hashimoto, "Conduction band energy level control of titanium dioxide: toward an efficient visible-light-sensitive photocatalyst," *Journal of the American Chemical Society*, vol. 132, no. 20, pp. 6898–6899, 2010.
- [5] H. Yu, J. Yu, B. Cheng, and S. Liu, "Novel preparation and photocatalytic activity of one-dimensional TiO₂ hollow structures," *Nanotechnology*, vol. 18, no. 6, Article ID 065604, 2007.
- [6] Y.-C. Liu, Y.-F. Lu, Y.-Z. Zeng, C.-H. Liao, J.-C. Chung, and T.-Y. Wei, "Nanostructured mesoporous titanium dioxide thin film prepared by sol-gel method for dye-sensitized solar cell," *International Journal of Photoenergy*, vol. 2011, Article ID 619069, 9 pages, 2011.
- [7] J. Šubrt, J. M. Criado, L. Szatmáry et al., "Mechanochemical synthesis of visible light sensitive titanium dioxide photocatalyst," *International Journal of Photoenergy*, vol. 2011, Article ID 156941, 9 pages, 2011.
- [8] J. Yao and C. Wang, "Decolorization of methylene blue with TiO₂ sol via UV irradiation photocatalytic degradation," *International Journal of Photoenergy*, vol. 2010, Article ID 643182, 6 pages, 2010.
- [9] N. Hafizah and I. Sopyan, "Nanosized TiO₂ photocatalyst powder via sol-gel method: effect of hydrolysis degree on powder properties," *International Journal of Photoenergy*, vol. 2009, Article ID 962783, 9 pages, 2009.
- [10] Z. Zhang and J. Gamage, "Applications of photocatalytic disinfection," *International Journal of Photoenergy*, vol. 2010, Article ID 764870, 11 pages, 2010.
- [11] H. Irie, S. Washizuka, N. Yoshino, and K. Hashimoto, "Visible-light induced hydrophilicity on nitrogen-substituted titanium dioxide films," *Chemical Communications*, vol. 9, no. 11, pp. 1298–1299, 2003.
- [12] A. Y. Nosaka, E. Kojima, T. Fujiwara, H. Yagi, H. Akutsu, and Y. Nosaka, "Photoinduced changes of adsorbed water on a TiO₂ photocatalytic film as studied by ¹H NMR spectroscopy," *Journal of Physical Chemistry B*, vol. 107, no. 44, pp. 12042–12044, 2003.
- [13] N. Sakai, A. Fujishima, T. Watanabe, and K. Hashimoto, "Enhancement of the photoinduced hydrophilic conversion rate of TiO₂ film electrode surfaces by anodic polarization," *Journal of Physical Chemistry B*, vol. 105, no. 15, pp. 3023–3026, 2001.
- [14] J. Yu and X. Zhao, "Effect of surface treatment on the photocatalytic activity and hydrophilic property of the sol-gel derived TiO₂ thin films," *Materials Research Bulletin*, vol. 36, no. 1-2, pp. 97–107, 2001.
- [15] J. Yu, J. C. Yu, W. Ho, and Z. Jiang, "Effects of calcination temperature on the photocatalytic activity and photo-induced super-hydrophilicity of mesoporous TiO₂ thin films," *New Journal of Chemistry*, vol. 26, no. 5, pp. 607–613, 2002.

- [16] Z. R. Tian, J. A. Voigt, J. Liu, B. McKenzie, and H. Xu, "Large oriented arrays and continuous films of TiO₂-based nanotubes," *Journal of the American Chemical Society*, vol. 125, no. 41, pp. 12384–12385, 2003.
- [17] H. Tokudome and M. Miyauchi, "Titanate nanotube thin films via alternate layer deposition," *Chemical Communications*, vol. 10, no. 8, pp. 958–959, 2004.
- [18] L. Zhao, J. Yu, J. Fan, P. Zhai, and S. Wang, "Dye-sensitized solar cells based on ordered titanate nanotube films fabricated by electrophoretic deposition method," *Electrochemistry Communications*, vol. 11, no. 10, pp. 2052–2055, 2009.
- [19] Y. Lai, Y. Chen, Y. Tang, D. Gong, Z. Chen, and C. Lin, "Electrophoretic deposition of titanate nanotube films with extremely large wetting contrast," *Electrochemistry Communications*, vol. 11, no. 12, pp. 2268–2271, 2009.
- [20] J. Yu and M. Zhou, "Effects of calcination temperature on microstructures and photocatalytic activity of titanate nanotube films prepared by an EPD method," *Nanotechnology*, vol. 19, no. 4, Article ID 045606, 2008.
- [21] Y. Wu, M. Long, W. Cai et al., "Preparation of photocatalytic anatase nanowire films by in situ oxidation of titanium plate," *Nanotechnology*, vol. 20, no. 18, Article ID 185703, 2009.
- [22] N.-H. Lee, H.-J. Oh, S.-C. Jung, W.-J. Lee, D.-H. Kim, and S.-J. Kim, "Photocatalytic properties of nanotubular-shaped TiO₂ powders with anatase phase obtained from titanate nanotube powder through various thermal treatments," *International Journal of Photoenergy*, vol. 2011, Article ID 327821, 7 pages, 2011.
- [23] L. Zhao, J. Ran, Z. Shu, G. Dai, P. Zhai, and S. Wang, "Effects of calcination temperatures on photocatalytic activity of ordered titanate nanoribbon/SnO₂ films fabricated during an EPD process," *International Journal of Photoenergy*, vol. 2012, Article ID 472958, 7 pages, 2012.
- [24] J. G. Yu, H. G. Yu, B. Cheng, and C. Trapalis, "Effects of calcination temperature on the microstructures and photocatalytic activity of titanate nanotubes," *Journal of Molecular Catalysis A*, vol. 249, no. 1-2, pp. 135–142, 2006.
- [25] H. G. Yu, J. G. Yu, B. Cheng, and J. Lin, "Synthesis, characterization and photocatalytic activity of mesoporous titania nanorod/titanate nanotube composites," *Journal of Hazardous Materials*, vol. 147, no. 1-2, pp. 581–587, 2007.
- [26] K. I. Ishibashi, A. Fujishima, T. Watanabe, and K. Hashimoto, "Detection of active oxidative species in TiO₂ photocatalysis using the fluorescence technique," *Electrochemistry Communications*, vol. 2, no. 3, pp. 207–210, 2000.
- [27] J. Yu, Q. Xiang, and M. Zhou, "Preparation, characterization and visible-light-driven photocatalytic activity of Fe-doped titania nanorods and first-principles study for electronic structures," *Applied Catalysis B*, vol. 90, no. 3-4, pp. 595–602, 2009.
- [28] G. S. Kim, V. P. Godbole, H. K. Seo, Y. S. Kim, and H. S. Shin, "Sodium removal from titanate nanotubes in electrodeposition process," *Electrochemistry Communications*, vol. 8, no. 3, pp. 471–474, 2006.
- [29] G. H. Du, Q. Chen, R. C. Che, Z. Y. Yuan, and L. M. Peng, "Preparation and structure analysis of titanium oxide nanotubes," *Applied Physics Letters*, vol. 79, no. 22, pp. 3702–3704, 2001.
- [30] Q. Chen, W. Zhou, G. H. Du, and L. M. Peng, "Trititanate nanotubes made via a single alkali treatment," *Advanced Materials*, vol. 14, no. 17, pp. 1208–1211, 2002.
- [31] R. Ma, Y. Bando, and T. Sasaki, "Nanotubes of lepidocrocite titanates," *Chemical Physics Letters*, vol. 380, no. 5-6, pp. 577–582, 2003.
- [32] H. Yu, J. Yu, and B. Cheng, "Facile preparation of Na-free anatase TiO₂ film with highly photocatalytic activity on soda-lime glass," *Catalysis Communications*, vol. 7, no. 12, pp. 1000–1004, 2006.
- [33] J. C. Yu, W. Ho, J. Lin, H. Yip, and P. K. Wong, "Photocatalytic activity, antibacterial effect, and photoinduced hydrophilicity of TiO₂ films coated on a stainless steel substrate," *Environmental Science and Technology*, vol. 37, no. 10, pp. 2296–2301, 2003.

